International Journal of Heat and Mass Transfer 53 (2010) 3977–3989

Contents lists available at ScienceDirect

International Journal of Heat and Mass Transfer

journal homepage: www.elsevier.com/locate/ijhmt

Numerical studies of simultaneously developing laminar flow and heat transfer in microtubes with thick wall and constant outside wall temperature

Sun-Xiao Zhang [a,b], Ya-Ling He [a], Guy Lauriat [c], Wen-Quan Tao [a,*]

[a] School of Energy and Power Engineering, State Key Laboratory of Multiphase Flow in Power Engineering, Xi'an Jiaotong University, Xi'an, Shaanxi 710049, PR China
[b] School of Environment Science and Engineering, Chang'an University, Xi'an, Shaanxi, PR China
[c] LETEM, Universite de Marne-la-Valle, France

ARTICLE INFO

Article history:
Received 15 July 2009
Received in revised form 9 April 2010
Accepted 9 April 2010
Available online 1 June 2010

Keywords:
Numerical studies
Thick wall microtube
The thermal entrance length
Axial heat conduction

ABSTRACT

The effects of wall axial heat conduction in a conjugate heat transfer problem in simultaneously developing laminar flow and heat transfer in straight thick wall of circular tube with constant outside wall temperature are numerically investigated. The results show that the heat transfer process is most sensitive to wall-to-fluid conductivity ratio k_{sf}, and when $k_{sf} \leqslant 25$ the increasing tube thickness and the decreasing k_{sf} could make the inner wall surface approaching the uniform heat flux condition. It turns out that the basic function of the wall axial heat conduction for the cases studied is to unify the inner wall surface heat flux.

1. Introduction

Conjugate heat transfer in laminar duct flow was widely analyzed in the last century. Since the entrance problem was first proposed by Graetz [1,2], a broad effort has been made to get information both on the thermal entrance region and on the fully developed region under different kinds of boundary conditions. A comprehensive review of the huge amount of results on the subject is available in the monograph by Shah and London [3]. One of the issues in the study of developing heat transfer in tubes or ducts is the effect of wall heat conduction. This subject is especially important when the heat transfer in microtubes is concerned. The small size in the spanwise direction in microtubes/ducts makes almost all microtubes/ducts be of thick-walled type. And this is the major concern of this paper. In the following only the references related to the effect of tube/duct wall heat conduction are briefly reviewed. Davis and Gill [4] analyzed the effect of axial wall conduction on the Couette flow between parallel plates. Mori et al. [5,6] investigated the effects of wall conduction on the convective heat transfer between parallel plates and in circular pipes under the boundary conditions of the first and the second kind. Faghri and Sparrow [7] investigated the simultaneous wall and fluid axial conduction in laminar pipe-flow heat transfer and proposed a criterion for judging the importance of the axial heat conduction. Zariffeh et al. [8] studied the combined effects of wall and fluid axial conduction on laminar heat transfer in circular tubes numerically. Campo and Rangel [9] analytically studied the conjugate effect of 1-D wall and fluid axial conduction. Barozzi and Pagliarini [10] investigated flow in thick-walled pipes with two-dimensional conduction analytically. Campo and Shuler [11] did lumped system analyses for the simultaneous wall and fluid axial conduction in laminar pipe flow heat transfer. Bilir [12] numerically analyzed the combined effect of 2-D (radial–axial) wall conduction and fluid conduction for low Peclet number ($Pe \leqslant 20$) fully developed laminar flow heat transfer in a thick-walled two-regional large circular pipe which has external constant temperature with a step change at a given section. Above-mentioned references were mostly published before the time when the so-called micro-heat transfer was emerging. And the major concerns of those papers are either the effect of one dimensional wall conduction or the combined effect of two-dimensional wall conduction and fluid axial conduction for low Peclet number duct laminar flow heat transfer with not very large ratio of wall thickness over tube diameter. During the last two decades the development of MEMS stimulated a great interest to study flow and heat transfer in microchannels [13,14].

One particular characteristic of convective heat transfer in mini-micro scale channels is its rather strong multi-dimensional character [14].

With the increasing of the ratio of the wall thickness over the hydraulic diameter, the coupling between the wall and the bulk fluid temperatures becomes more important, and the axial conduction through the tube wall has to be considered very seriously. In [15] numerical simulation was made for a circular thick tube with

* Corresponding author. Tel./fax: +86 29 82669106.
E-mail address: wqtao@mail.xjtu.edu.cn (W.-Q. Tao).

0017-9310/$ - see front matter © 2010 Elsevier Ltd. All rights reserved.
doi:10.1016/j.ijheatmasstransfer.2010.05.017

Nomenclature

c_p	specific heat of fluid, J/(kg K)
d_i	inner diameter of tube, m
f	friction factor
k	thermal conductivity, W/(m K)
k_{sf}	wall-to-fluid thermal conductivity ratio
L	total length of tube, m
L_H	theoretical hydrodynamic entrance length, m
L_T	theoretical thermal entrance length, m
Nu	Nusselt number
Pr	Prantl number
q_r	reference heat flux, W/m^2
$q_{w,in,x}$	non-dimensional inner interfacial heat flux
r	radial coordinate, m
R	non-dimensional radial coordinate
Re	Reynolds number
Pe	Peclet number Pe = RePr
t	temperature, K
T	non-dimensional temperature
u	velocity in the axial direction
U	non-dimensional velocity in the axial direction
v	velocity in the radial direction
V	non-dimensional velocity in the radial direction
x	axial coordinate, m
X	non-dimensional axial coordinate

Greek symbol

ρ	fluid density, kg/m^3
η	dynamic viscosity, Pa s
δ	non-dimensional wall thickness

Subscripts

f	fluid
fb	cross-section mean value
i	inner surface of tube
in	inlet
o	outer surface of tube
s	solid
w	outer wall surface of tube
wi	inner wall surface of tube
∞	limiting value far down the duct

third kind of outside boundary condition with different thermal conductivity ratio of wall to fluid. Their results show that the larger thermal conductivity ratio leads to a lower Nusselt number in the laminar fully developed region and the very low ratio approximate the constant wall heat flux, which is consistent with the results obtained by Sparrow and Patankar [16]. The numerical results in [15] also show that the fully developed Nusselt number decreases with the decrease in the ratio of outer over inner tube diameters. Maranzana et al. [17] have analyzed the influence of the axial conduction in the tube wall on microchannels and proposed a non-dimensional number (M) to quantify the effect of axial conduction in walls. Zueco et al. [18] analyzed a thick-walled macro-tube with a step change outside temperature by network method. They concluded qualitatively that the effect of wall conduction on heat transfer increases as the Peclet number and thermal conductivity ratio of solid wall over fluid decrease. Tiselj et al. [19] studied the effect of axial conduction on the water heat transfer in multi-micro-channels with triangle cross section. Gamrat et al. [20] studied the flow and heat transfer in a micro-channel by both experimental and numerical methods. They concluded that there is no size effect on heat transfer when the channel spacing is reduced from 1.0 mm down to 0.1 mm. The strong reduction in the Nusselt number observed in experiments cannot be explained by axial conduction in the walls or lack of two-dimensionality of the heat flux distribution. Further investigations are needed in order to reduce the gap between the results of some experiments and numerical simulation. Hetsroni et al. [21] studied water heat transfer in a multi-micro-channel and found that for the cases studied the viscous dissipation can be ignored. Bavière et al. [22] studied the bias effects on heat transfer measurements in microchannel flows. It is concluded that a bias effect on the solid/fluid interface temperature measurement may account for the apparent scale effects observed in some references. Celata et al. [23] experimentally measured the heat transfer characteristics in micro tube uniformly heated with inner diameter ranging from 50 μm to 528 μm. They found some decrease in heat transfer performance with respect to the conventional value (Nu = 4.36) and it is more marked for decreasing Reynolds number. They attributed this reduction to a heat loss term. Lelea [24] studied the conjugate heat transfer of water in partially heated microchannels by numerical method. Three different tube wall materials were considered, stainless steel (k = 15.9 W/m K), silicon (k = 189 W/m K) and copper (k = 398 W/m K). Two different cases of the partial Joule heating were considered for the tube wall. The local Nu exhibits the usual distribution as for the non-axial conduction case, and the local Nusselt number at fully developed region has the usual value of 4.36. In [25] experimental measurements were conducted for heat transfer in three microtubes with different thickness over diameter ratio and uniformly heated outside. Their results show that with the increase in Reynolds number the local Nusselt number in the downstream region approaches 4.36. Liu et al. [26] experimentally studied the effect of axial wall heat conduction for convective heat transfer in stainless steel microtube with Joule heating. Distilled water and nitrogen gas were used as the working fluids flow through the stainless steel microtube with inner diameter 168 μm and outer diameter 406 μm. The wall temperature field photos of the microtube are acquired by employing an IR camera. Their results show that the axial heat conduction can reduce the convective heat transfer in the stainless steel microtube and the decrement may reach 2% compared to the convective heat transfer when the working fluid is nitrogen gas, however, the decrement can be neglected for distilled water as the working fluid. Weigand and Gassner [27] investigated the effect of wall conduction for the extended Graetz problem for laminar and turbulent channel flows with a thick-walled model numerically. The channel wall only has a small part located in the center being kept at high temperature while the rest at lower temperature. The heat conduction within the solid wall changes the temperature distribution at the interface between the solid and the fluid. The increasing in solid wall thermal conductivity leads to reducing the abrupt temperature change at the interface.

From above review, it can be seen that even though a great number of numerical and experimental studies have been performed on the wall heat conduction effect on the entrance problem in mini/microchannels or tubes, we still have not a very clear picture on what is the effect of the wall axial heat conduction? With what condition the effect of the axial heat conduction can be neglected? And if the axial heat conduction is very severe, what will be the result? Because of the complexity of heat transfer in micro-channel or tube situation, we may first pay attention to a very simple, yet typical and interesting problem in heat transfer theory as follows: fluid with uniform velocity and temperature flowing into a thick-walled tube with a constant temperature of its outside surface. The two ends of the tube are adiabatic. For that case the negligible axial heat conduction leads to uniform temperature of the inner surface, and hence the fully developed Nusselt number should be 3.66. If the axial heat conduction plays a role, then the inner surface of the wall will depart from the uniform wall surface condition. By using this model the above-referenced three problems can be clearly answered. This is the major purpose of the present paper.

In this paper in order to clarify the above-mentioned three questions, the conjugate effect of two-dimensional wall conduction (both radial and axial) and fluid axial conduction is analyzed for simultaneously developing laminar flow and heat transfer in a microtube with the ratio of wall thickness over tube diameter varying in a wide range and a constant outer surface temperature.

It should be noted that even though the problem studied here seems to be quite simple in both governing equation and boundary conditions, the three questions listed above are remained unsolved in the literatures. To obtain their correct answers is not only just for academic purpose, but also is meaningful for development of theory of MEMS design. Even though many commercial softwares are available, readers do not know the code details of implementation of some numerical treatments. And sometimes a minor difference in code implementation may lead to different results. In order to make sure that every our numerical treatments is correctly coded, we use a self-developed code to perform numerical simulation. Such practice was adopted in [24,28,29].

2. Numerical analysis

The physical problem investigated is as follows. A fluid with a temperature t_{in} and velocity u_{in} is going into a circular tube of inner diameter d_i and wall thickness $(r_o - r_i)$ with its outside surface temperature being at constant value t_w. The tube is assumed to be long enough. The velocity and temperature fields at different ratio of wall thickness over inner diameter and different thermal conductivity ratio of wall over fluid are searched for. Fig. 1 presents the computational domain.

As indicated in [30] for fluid flows in microchannels with Knudsen number less than 0.001 the continuum model is still valid. Thus the 2-D steady Navier–Stokes and energy equations are used to describe the flow and heat transfer in the whole region. The following assumptions are adopted: (1) The fluid is incompressible and the fluid flow is in steady state; (2) The flow is laminar; (3) The radiation heat transfer is neglected; (4) The body force is neglected; (5) The electrostatic force is neglected [25]; (6) The thermal properties of solid and fluid are assumed to be constant. Based on the above assumptions the problem to be investigated is axisymmetrical and the governing equations are as follows:

Continuity

$$\rho_f \frac{\partial u}{\partial x} + \rho_f \frac{1}{r}\frac{\partial (rv)}{\partial r} = 0 \tag{1}$$

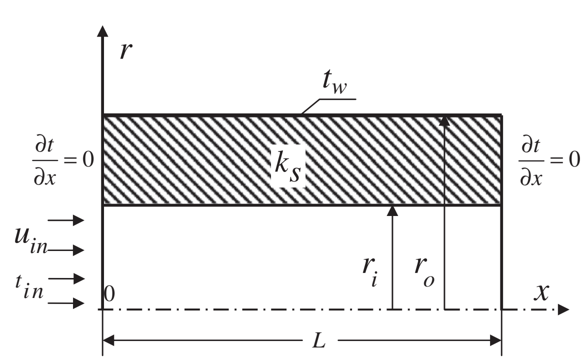

Fig. 1. The computational domain of convective heat transfer in thick wall tube.

Momentum

$$\frac{\partial(\rho_f uv)}{\partial x} + \frac{1}{r}\frac{\partial(\rho_f uv)}{\partial r} = -\frac{dp}{dx} + \frac{\partial}{\partial x}\left(\eta_f \frac{\partial u}{\partial x}\right) + \frac{1}{r}\frac{\partial}{\partial r}\left(r\eta_f \frac{\partial u}{\partial r}\right) \tag{2}$$

$$\frac{\partial(\rho_f uv)}{\partial x} + \frac{1}{r}\frac{\partial(rvv)}{\partial r} = -\frac{dp}{dr} + \frac{\partial}{\partial x}\left(\eta_f \frac{\partial v}{\partial x}\right) + \frac{1}{r}\frac{\partial}{\partial r}\left(r\eta_f \frac{\partial v}{\partial r}\right) - \eta_f \frac{v}{r^2} \tag{3}$$

Energy

liquid
$$\frac{\partial(\rho_f c_{p,f} u t_f)}{\partial x} + \frac{1}{r}\frac{\partial(r\rho_f c_{p,f} v t_f)}{\partial r} = \frac{\partial}{\partial x}\left(k_f \frac{\partial t_f}{\partial x}\right) + \frac{1}{r}\frac{\partial}{\partial r}\left(rk_f \frac{\partial t_f}{\partial r}\right) \tag{4}$$

solid
$$\frac{\partial}{\partial x}\left(k_s \frac{\partial t_s}{\partial x}\right) + \frac{1}{r}\frac{\partial}{\partial r}\left(rk_s \frac{\partial t_s}{\partial r}\right) = 0 \tag{5}$$

It can be seen from Eqs. (4) and (5) that the tube wall can be treated as a special fluid with very large dynamic viscosity. Such computational treatment makes the problem being conjugated [31,32] and can greatly simplify the computation. This practice is adopted in this paper.

The two ends of the tube wall are assumed to be adiabatic, and at the exit of the computation domain, the fully developed condition is adopted. Thus all the boundary conditions can be mathematically expressed as follows:

$$\begin{aligned}
&x=0, \quad 0 \leqslant r \leqslant r_i, \quad u = u_{in}, \quad v=0, \quad t_f = t_{in}\\
&x=0, \quad r_i \leqslant r \leqslant r_o, \quad u=v=0, \quad \frac{\partial t_s}{\partial x}=0\\
&x=L, \quad 0 \leqslant r \leqslant r_i, \quad \frac{\partial u}{\partial x}=0, \quad \frac{\partial t_f}{\partial x}=0\\
&x=L, \quad r_i \leqslant r \leqslant r_o, \quad u=v=0, \quad \frac{\partial t_s}{\partial x}=0\\
&r=0, \quad 0 \leqslant x \leqslant L, \quad \frac{\partial u}{\partial x}=0, \quad v=0, \quad \frac{\partial t_f}{\partial r}=0\\
&r=r_0, \quad 0 \leqslant x \leqslant L, \quad u=0, \quad v=0, \quad t_s = t_w
\end{aligned} \tag{6}$$

In order to generalize the solution results, the above governing equations and the boundary conditions are non-dimensionalized as follows:

$$\frac{\partial U}{\partial X} + \frac{1}{R}\frac{\partial(RV)}{\partial R} = 0 \tag{7}$$

$$\frac{\partial(UU)}{\partial X} + \frac{1}{R}\frac{\partial(RUV)}{\partial R} = -\frac{\partial P}{\partial X} + \frac{\partial}{\partial X}\left(\frac{2}{\mathrm{Re}}\frac{\partial U}{\partial X}\right) + \frac{1}{R}\frac{\partial}{\partial R}\left(R\frac{2}{\mathrm{Re}}\frac{\partial U}{\partial R}\right) \tag{8}$$

$$\frac{\partial(UV)}{\partial X} + \frac{1}{R}\frac{\partial(RVV)}{\partial R} = -\frac{\partial P}{\partial R} + \frac{\partial}{\partial X}\left(\frac{2}{\mathrm{Re}}\frac{\partial V}{\partial X}\right) + \frac{1}{R}\frac{\partial}{\partial R}\left(R\frac{2}{\mathrm{Re}}\frac{\partial V}{\partial R}\right) - \frac{2}{\mathrm{Re}}\frac{V}{R^2} \tag{9}$$

$$\frac{\partial(UT_f)}{\partial X} + \frac{1}{R}\frac{\partial(RVT_f)}{\partial R} = \frac{\partial}{\partial X}\left(\frac{2}{\mathrm{RePr}}\frac{\partial T_f}{\partial X}\right) + \frac{1}{R}\frac{\partial}{\partial R}\left(\frac{2}{\mathrm{RePr}}R\frac{\partial T_f}{\partial R}\right) \tag{10}$$

$$\frac{\partial}{\partial X}\left(\frac{k_s}{k_f}\frac{2}{\mathrm{RePr}}\frac{\partial Ts}{\partial X}\right) + \frac{1}{R}\frac{\partial}{\partial R}\left(\frac{k_s}{k_f}\frac{2}{\mathrm{RePr}}R\frac{\partial Ts}{\partial R}\right) = 0 \tag{11}$$

$$\begin{aligned}
&X=0, \quad 0 \leqslant R \leqslant 1.0, \quad U=1.0, \quad V=0.0, \quad T_f=0\\
&X=0, \quad 1.0 \leqslant R \leqslant R_o, \quad U=V=0, \quad \frac{\partial T_s}{\partial X}=0\\
&X=\frac{L}{r_i}, \quad 0 \leqslant R \leqslant 1.0, \quad \frac{\partial U}{\partial X}=0, \quad \frac{\partial T_f}{\partial X}=0
\end{aligned}$$

$$X=\frac{L}{r_i},\quad 1.0\leqslant R\leqslant R_o,\quad U=V=0,\quad \frac{\partial T_s}{\partial X}=0$$
$$R=0,\quad 0\leqslant X\leqslant \frac{L}{r_i},\quad \frac{\partial U}{\partial X}=0,\quad V=0,\quad \frac{\partial T_f}{\partial R}=0$$
$$R=R_0,\quad 0\leqslant X\leqslant \frac{L}{r_i},\quad U=0,\quad V=0,\quad T_S=1 \tag{12}$$

The non-dimensional variables are defined as

$$X=x/r_i,\quad R=r/r_i\quad U=u/u_{in},\quad V=v/u_{in},\quad T=(t-t_{in})/(t_w-t_{in})$$

It should be noted that the energy equations for fluid and tube wall are deliberately expressed in separated way (Eqs. (10) and (11)) in order to show the different thermal conductivity ratios. During the numerical simulation the fluid and tube wall are treated by the same equation with different thermo-physical properties.

The finite-volume-method (FVM) [29–32] is used to discretize the governing equations, the SGSD scheme [33,31] is used for the discretization of the convective term, and the SIMPLEC algorithm [34,32] is adopted to deal with the linkage between velocity and pressure. The whole region (including the solid wall) is treated as the computational domain. The total length of x-direction is taken as 5 times of the entrance length theoretically determined for the tube of conventional size.

A preliminary computation has been conducted to determine the grid system which can guarantee to obtain the grid-independent solutions. Satisfactory results are obtained by using a grid spacing number of 16–62 in the r-direction with 16 in the fluid region and 0–46 in the solid according to the wall thickness. A total number of grid spacing in the x-direction is determined according to the ratio of length to width being taken, in which the grid spacing is ranged from one to four times of the grid spacing in the radial direction. The computation is of conjugated type. The numerical method for such conjugated computation is well documented in Refs. [29–32], and will not be re-stated here. The iterations are continued until convergence up to the fifth digit of both velocity and temperature is achieved.

With the converged velocity and temperature fields, the local Poiseuille number (fRe), the non-dimensional bulk temperature, the non-dimensional inner interfacial heat flux and Nusselt number can be defined as follows:

$$(f\mathrm{Re})_x=-16\left(\frac{\partial U}{\partial R}\right)_{R=1} \tag{13}$$
$$T_{fb}=\frac{\int_0^1 UT_f R dR}{\int_0^1 URdR} \tag{14}$$
$$q_{w,in,x}=\left(\frac{\partial T_f}{\partial R}\right)_{R=1} \tag{15}$$
$$Nu_x=\frac{2}{T_{wi}-T_{fb}}\left(\frac{\partial T_f}{\partial R}\right)_{R=1}=\frac{2q_{w,in,x}}{T_{wi}-T_{fb}} \tag{16}$$

In Eq. (16) the temperature difference between inner wall and fluid bulk temperature is used for the local heat transfer coefficient and this is a usual practice in heat transfer community. Especially for the cases studied, the outside wall temperature remains constant. It is the inner wall temperature that can reflect the effect of axial wall heat conduction.

In addition, the Reynolds number is defined as follows:

$$\mathrm{Re}=2r_i u_{in}\rho_f/\eta_f \tag{17}$$

The theoretical hydrodynamic and thermal entrance lengths are respectively as follows [35]:

$$L_H=0.1\mathrm{Re}_D R_i \tag{18a}$$
$$L_T=0.1\mathrm{Re}_D \mathrm{Pr} R_i \tag{18b}$$

Table 1
Parameters of numerical simulations.

Re	Pr	k_{sf}	δ/R_i
10, 30, 50, 100, 200, 2000, 2280	1, 3, 5, 7	1, 10, 15, 25, 50, 100, 300, 500, 664, 10,000	0, 0.08, 0.42, 0.84, 1.69, 2.53, 3.37, 3.79

Table 2
Typical values of the thermal conductivity ratio k_{sf} at 20 °C.

	Water	Air	Oil
Copper	665	15,960	2660
Aluminum	393	9440	1573
Iron	135	3240	540
Steel	23	560	93
Glass	1.67–1.84		
PMMA	0.33		
PDMS	0.33		
Quartz	2.34		

These two quantities will be referred in the later discussion.

Numerical simulations are performed in a wide range of parameter variations, as shown in Table 1. The typical values of the thermal conductivity ratio k_{sf} at 20 °C are indicated in Table 2. From the non-dimensional formulations of the governing equation, it can be found that the results of the problem depend on four parameters, Re, Pr, k_{sf} and δ/R_i. Simulations are grouped according to the four parameters. As can be seen from Table 2, the thermal conductivity ratio may be as large as 10^4 for the combination of copper over air, and may be as small as 1 for the combination of glass over water. In the study of conjugate convective heat transfer in microtubes the upper limit of the solid/fluid thermal conductivity ratio is usually taken quite high [36]. Thus apart from the wide variation ranges of Re and Pr, the thermal conductivity ratio of solid wall over fluid ranges from 1 to 10,000, and the largest ratio of wall thickness over the inner diameter up to 3.79. Such great value of δ/R_i can be found in the flows of mini/microchannels.

3. Results and analysis

As the validation of our self-coded program, the numerical results of the variation of $(f\mathrm{Re})_x$ and Nu_x versus $X/(R_i\mathrm{Re})$ when $\delta/R_i=0$ are presented in Fig. 2. It is shown that the numerically predicted hydrodynamic and thermal entrance lengths, the fully developed Poiseuile number and Nusselt number coincide with the conventional results ($L_H/R_i\mathrm{Re}=0.1$, $L_T/R_i\mathrm{Re\,Pr}=0.1$, $(f\mathrm{Re})_\infty=64$, $Nu_\infty=3.66$) very well when the grid points in the fluids at the radial direction are taken as 20. The relative differences between simulated values and analytical values are listed in Table 3.

In the following fours figures are used to present major numerical results. (1) The variations of the dimensionless local heat flux at the inner wall at different combination of Re, Pr and k_{sf} are shown in Fig. 3; (2) The streamwise variation patterns of the inner surface temperature with the k_{sf} are provided in Fig. 4; (3) In Fig. 5 the variation pattern of local fluid bulk temperature with axial distance at different combination of Re, Pr and k_{sf} are presented; (4) The effect of tube wall thickness and the fluid Peclet number on the variation of local Nusselt number with axial distance is expressed in Fig. 6.

In Fig. 3 six figures are presented for the variation of the dimensionless local heat flux at the inner wall at different combination of Re, Pr and k_{sf}. The six figures can be grouped into three categories, in each category the first figure represents the results for the smallest value of k_{sf}(=1), while the other figure is for $k_{sf}=25$. It is clear that k_{sf} is a key parameter influencing the distribution pattern of

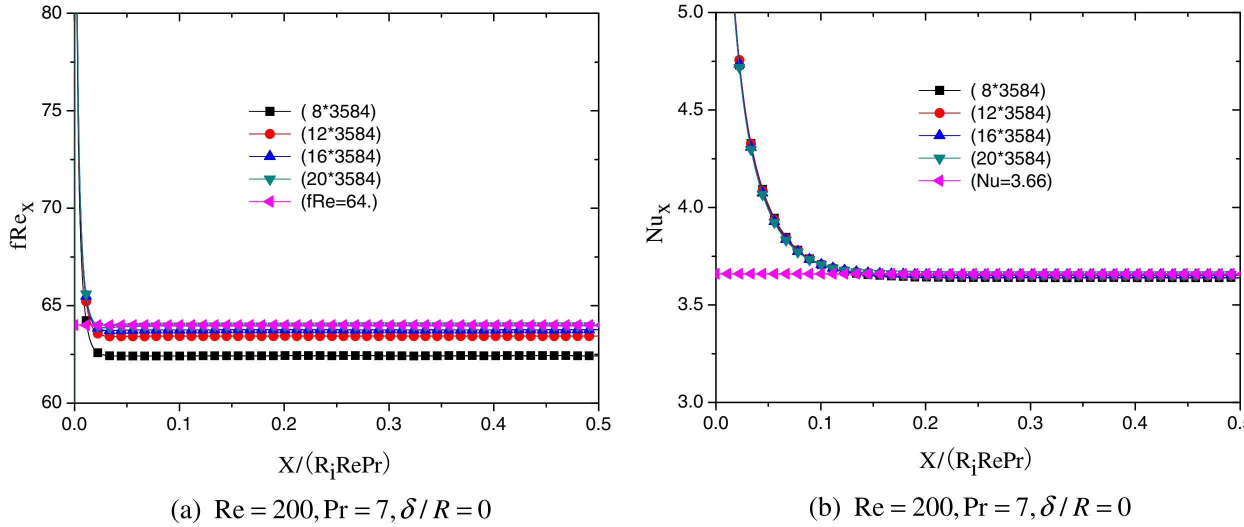

Fig. 2. Relation between local value $(f\mathrm{Re})_x$ and Nu_x and the grid points in fluid domain.

Table 3
Effects of radial grid number in fluids on simulation results

Grid numbers of the radial direction	Simulation error (%)	
	$\Delta(f\mathrm{Re})/(f\mathrm{Re})_\infty$	$\Delta Nu/(Nu)_\infty$
8	−2.47	−0.41
12	−0.88	−0.25
16	−0.38	−0.06
20	−0.07	+0.06

the local inner heat flux. When the value of k_{sf} is larger than 25, due to the higher wall thermal conductivity, the thermal resistance of wall radical heat conduction is negligible and the inner wall of the tube is actually experienced the constant temperature condition as the case of zero wall thickness. However, when k_{sf} is equal to or smaller than 25, the resistance of wall radical heat conduction is not negligible which makes the inner surface of the tube experienced a condition somewhat deviating from constant temperature situation. As can be seen from the second figure of each category when $k_{sf} = 1$, the inner wall surface heat flux has already exhibited a trend of approaching the uniform wall heat flux condition. And in that case the heat transfer process between the fluid and the inner wall surface is actually governed by the boundary condition of constant heat flux, even though the outside surface is at constant temperature condition.

Fig. 4 presents the streamwise variation pattern of the inner surface temperature with the value of k_{sf}. The six figures can be grouped into three categories, with each category being at the same Re and Pr but different k_{sf}. When the value of k_{sf} is equal to or smaller than 25, with the increasing tube wall thickness the effect of the wall axial heat conduction increases and the non-uniformity of the streamwise temperature profile of the inner wall surface becomes more severe and severe, which corresponds to the increasing uniformity of the inner surface heat flux. Figs. 4(a), (c) and (e) present such variation trend for the cases of $k_{sf} = 1$. As can be seen there the difference in the fluid Peclet number only makes some minor deviations between the temperature profiles of different δ/R_i, but does not have a quantitative effect on the inner surface temperature profiles. However, when the value of k_{sf} is larger than 25, the inner surface temperatures become more or less uniform and the influence of the tube wall thickness on the inner wall surface temperatures profile becomes insignificant.

In Fig. 5 the variation patterns of local fluid bulk temperature with axial distance at different combination of Re, Pr and k_{sf} are shown. Again the six pictures can be grouped into three categories, and in each category the difference between the two pictures is only at the value of k_{sf}: one for $k_{sf} = 1$ and the other for $k_{sf} = 25$. It is clear that k_{sf} is a key parameter influencing the streamwise fluid bulk temperature distribution. When the value of k_{sf} is equal to 1 (Figs. 5(a), (c) and (e)) with the increasing tube wall thickness the effect of the wall axial heat conduction increases, and the streamwise fluid bulk temperature profile varies from an exponential-like curve to nearly a linear one, which corresponds to the situation of uniform local heat flux at the inner surface, see the counterpart in Fig. 3.

Attention is now turned to the effect of tube wall thickness and the fluid Peclet number on the variation of local Nusselt number with axial distance. Fig. 6 shows the effects of tube wall thickness. As stated before, the value of k_{sf} is a key parameter to represent the influence of the axial wall heat conduction. Figs. 6(a), (c) and (e) clearly show that for the case of $k_{sf} = 1$, the local Nusselt number decreases sharply from an extremely high value at the very inlet of the tube to a constant value in the far downstream. All the eight variation curves are limited by two tube wall thicknesses: when the tube wall thickness approaches zero, the value of Nu_x in the far downstream region is 3.66, while for the very high tube wall thickness of $\delta/R_i = 3.79$ the far downstream value of Nu_x is about 4.3. However, if the value of $k_{sf} = 25$, then the difference between different tube wall thickness almost diminishes, and all the curves of different tube wall thickness emerge to one curve. The larger the fluid Peclet number the stronger such emerging trend. From our numerous computational results it is found that within the Peclet number range of 30–11,560 when the value of k_{sf} is smaller than 25, the variations of the local Nusselt number with tube wall thickness and Peclet number are more or less the same as the ones shown for $k_{sf} = 1$, while if the value of k_{sf} is greater than 25, the curves for different tube wall thickness soon emerge into one with a stronger trend as shown for $k_{sf} = 25$. In addition, as can be seen from Fig. 6, the thermal entrance length of a thicker tube wall is larger than the case of zero tube wall thickness, and the larger the ratio of wall thickness over tube inner diameter, the bigger the departure between them. In our numerical simulations the maximum departure between the two thermal entrance lengths exceeds 20%. However, when the value of k_{sf} is larger than 25, the maximum departure in the thermal entrance length is smaller

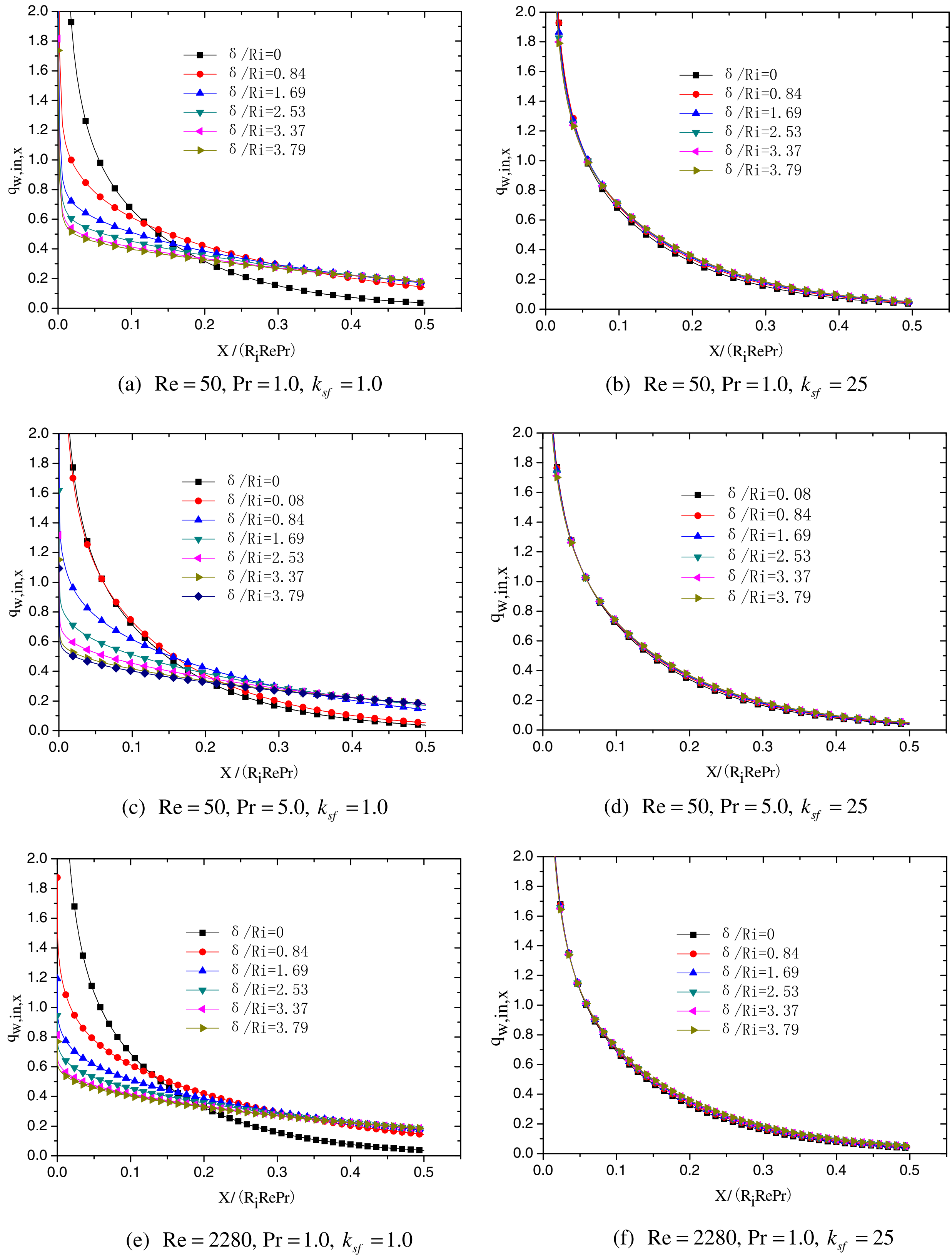

Fig. 3. Variation of local inner wall surface heat flux $q_{w,in,x}$ with non-dimensional distance $X/(R_i\text{RePr})$.

than 2%. From the examination of numerical results shown in Fig. 6, it can be concluded that depending on the thermal conductivity ratio the local Nusselt number in the fully developed region varies between two limits: from 3.66 for the constant wall surface condition to about 4.36 for the uniform wall heat flux condition.

It is interesting to note that Sparrow and Patankar [16] had made a complete analysis for the thermally developed duct flow with external convection under the conditions of negligible effect of the wall thickness. It shows that the constant wall temperature boundary condition and the constant wall heat flux boundary

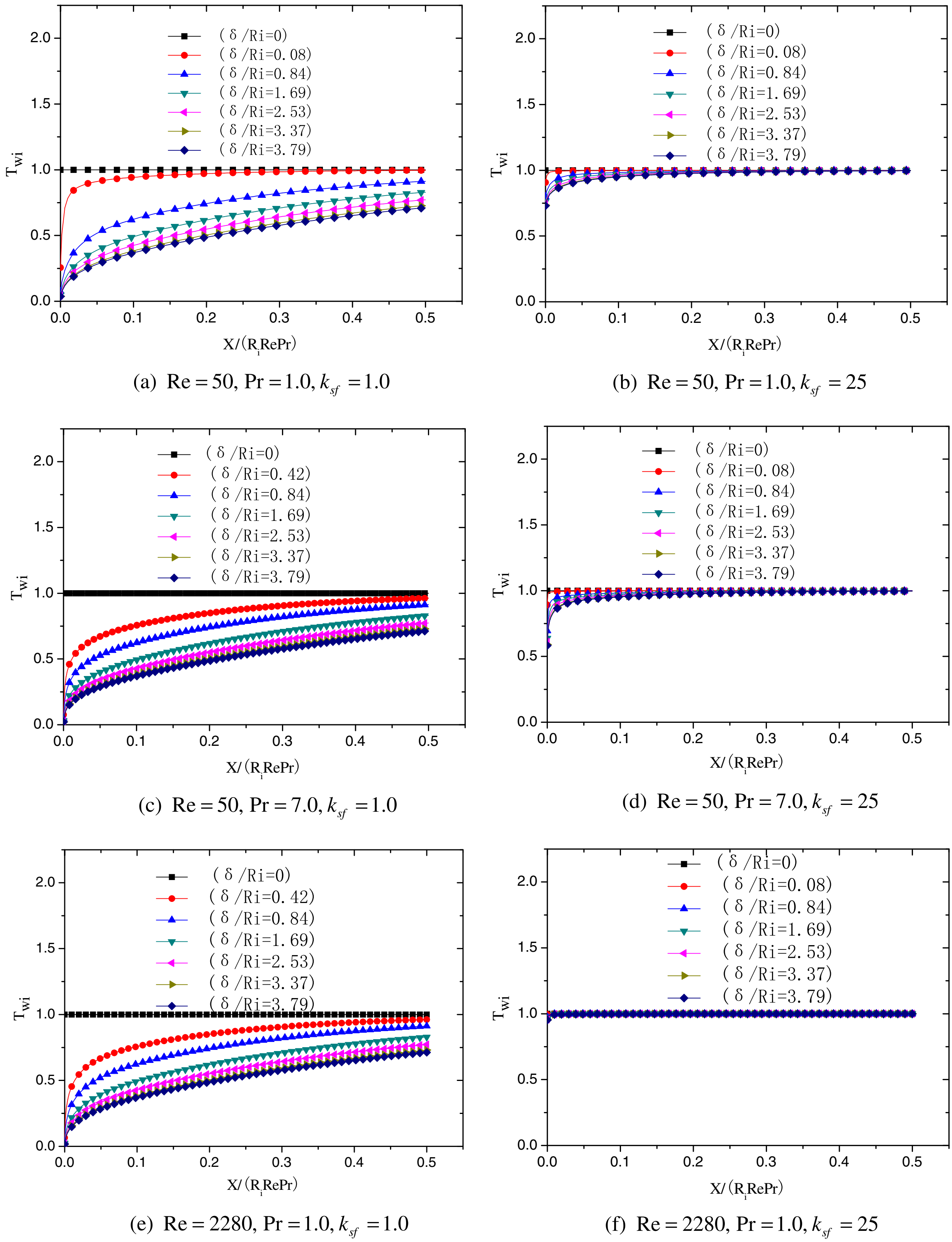

Fig. 4. Variation pattern of local inner surface temperature with non-dimensional streamwise distance $X/(R_i\mathrm{RePr})$.

condition are respectively of two extreme boundary conditions of thermally developed duct flow with external convection. When the external convective heat transfer coefficient is very large the Nusselt numbers in the thermally developed region reach 3.66, while when the external convective heat transfer coefficient is extremely small, the fully developed Nusselt number approaches 4.36.

In this paper, numerical results of our numerous simulations show that as the wall-to-fluid thermal conductivity ratio decreases and the ratio of wall thickness over tube diameter increases, the

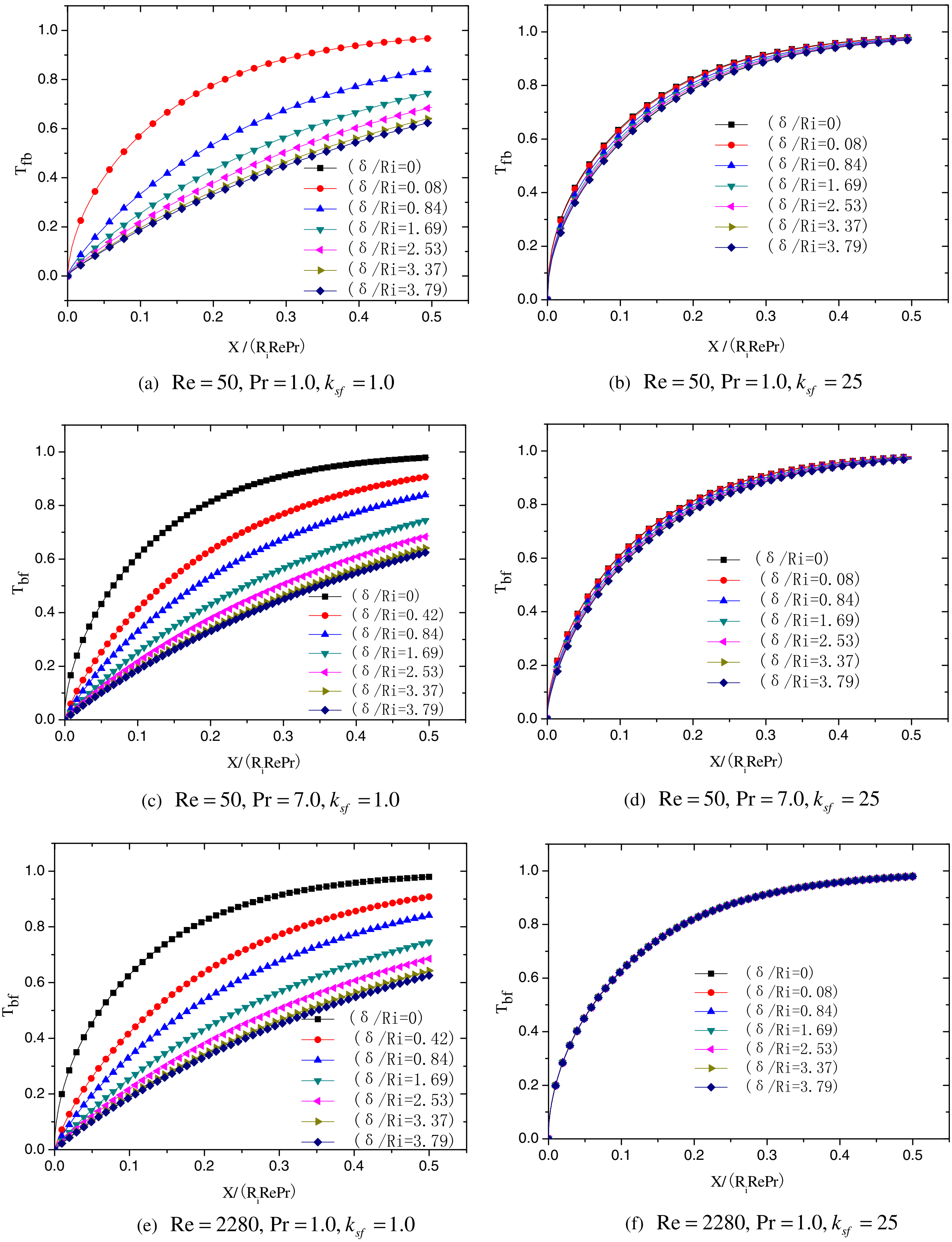

Fig. 5. Variation of local value T_{fb} with non-dimensional distance $X/(R_i\mathrm{RePr})$.

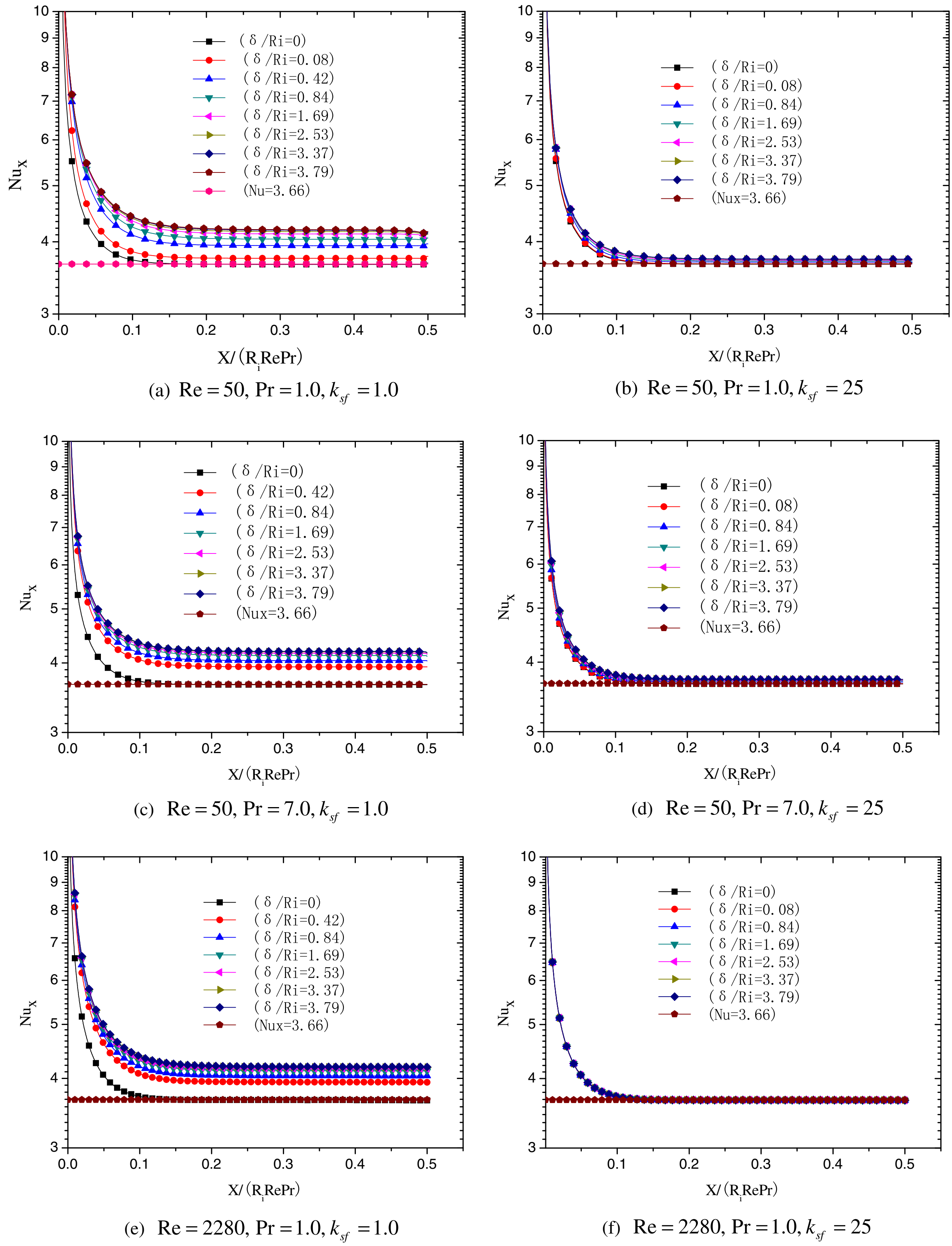

Fig. 6. Effect of tube wall thickness on the variation of Nu_x with $X/(R_i RePr)$.

convective heat transfer at the inner surface of a thick wall tube with constant temperature of the outside surface actually experiences a boundary condition transformation: from the constant wall temperature condition to the constant wall heat flux condition. To the authors' knowledge such clear statement and conclusion on the effect of the tube wall thickness is seemingly first in the literatures. And the discussion and comparison in the following section will provide some support to the above observation.

4. Discussion and comparison

4.1. What is the basic function of axial heat conduction?

From above presentation of our numerical results, it is quite clear that the basic function of the wall axial heat conduction for the case studied is to unify the heal flux at the inner surface of the tube. From our numerical study when k_{sf} is larger than 25, the axial heat conduction becomes so strong that influences from other parameters may be neglected. If k_{sf} is less than this value then other parameters, including the ratio of wall thickness over radius, the values of Re and Pr (i.e., the Peclet number) will have their effects. This thought can be very well understood from the physical intuition of transport phenomenon. This thought also can be qualitatively validated from the results of following references.

In the work of [24], the conjugate heat transfer of the water flow inside the microtubes (Di/Do = 0.1/03 mm and 0.1/0.5 mm) was investigated. Joule heating was used to study the tube wall conduction effect for three thermal conductivities: stainless steel (k = 15.9 W/m K), silicon (k = 189 W/m K) and copper (k = 398 W/m K). Two situations were studied: in one case the left half portion of the tube was uniformly heated and the right half portion was insulated, in the other case situation was the opposite. The local Nu exhibits the usual distribution as for the case with entire tube uniformly heated, and the local Nusselt number at fully developed region has the usual value of 4.36. Since the basic function of axial heat conduction is to unify the local heat flux. In the study of [24] the heat flux is already uniform in the heated portion, and the strong axial heat conduction caused by the large values of k_{sf} of the three combinations of solid/fluid further unify the heat flux such that in the inner surface the local Nusselt distribution is the same as the uniform heating for the entire tube.

In [27] only at the central small part of the tube surface the temperature is higher and constant and the rest part is at a lower and constant temperature. The heat conduction within the solid wall changes the temperature distribution at the interface between the solid and the fluid. The increasing values of the wall thickness over tube diameter ratio lead to flatting wall temperature and fluid bulk temperature distributions. This also implies that the increased axial heat conduction plays a role of unifying the streamwise heat flux.

Further supports can also be found from [37–39]. In [38] a circular tube was heated non-uniformly with the maximum heat flux at the middle location and the heat flux being lineally deceased towards the tube two ends. Numerical simulation by Fluent found that with the decreasing of fluid velocity the tube inner wall temperature of the downstream portion gradually increased and the whole axial distribution of the inner wall moved towards the linear distribution, which is the indication of uniform heat flux at the inner surface. In [39] a rectangular channel with certain thickness was heated only from bottom surface and the rest three surfaces were all adiabatic. The solid/fluid combination is copper and water, implying a very larger k_{sf}. Numerical simulation results by Fluent showed that the average Nusselt numbers simulated by 3-D conjugated model and a so-called "thin-wall" model of Fluent were in excellent agreement. The thin-wall model is a simplified 2-D model which essentially combines the uniform circumferential wall temperature and uniform heat flux conditions. This by no means that the axial heat conduction can be negligible, in the opposite, it is the strong axial heat conduction which makes the channel inner surfaces being at uniform heat flux that makes the thin-wall model applicable.

4.2. Criterion for judging effect of axial heat conduction may be situation dependent

As indicated above, Maranzana et al. [17] analyzed the influence of the axial conduction in the tube wall on microchannels and proposed a non-dimensional number (M) to quantify the effect of axial wall conduction. However, their analysis was based on the assumption of constant inner wall heat transfer coefficient which was prespecified; hence their results can not be applied to the entrance problem where the local heat transfer coefficient is a dependent variable rather than a given value. The non-dimensional number (M) is defined as follow [17]:

$$M = \frac{\phi_{cond//}}{\phi_{conv}} = \frac{r^2 NTU}{Bi} \tag{19}$$

where $\phi_{cond//}$ is a heat flux that characters axial heat transfer in the wall, ϕ_{conv} is the total convective heat flux, and the same temperature difference was used for the calculation of $\phi_{cond//}$ and ϕ_{conv}. It was stated in [17] that if the value of M is less than 10^{-2} the axial heat conduction effect may be neglected.

In [25] the temperature difference in calculating wall heat conduction and fluid convective heat transfer are adopted individually:

$$M = \frac{\phi_{cond//}}{\phi_{conv}} = \frac{A_{c,o}k_s\Delta t_s/L}{A_{c,i}\rho c_p u_{in}\Delta t_f} = \frac{2k_{sf}(R_o^2-1)\Delta t_s}{\mathrm{RePr}_f\Delta t_f(L/r_i)} \tag{20}$$

where

$$A_{c,o} = \pi(r_o^2 - r_i^2) \quad \text{and} \quad A_{c,i} = \pi r_i^2 \tag{21}$$

$$\Delta t_f = t_{fb} - t_{in}, \quad \Delta t_s = t_{s,o,ave} - t_{s,in,ave} \tag{22}$$

where $t_{s,o,ave}$, $t_{s,in,ave}$ are the outlet and inlet cross section average temperature of the tube, which is more suitable for the estimation of axial heat conduction along the wall.

From our numerical results it has been clearly demonstrated that for the cases studied if the thermal conductivity ratio (k_{sf}) is larger than 25, the wall thickness effect can be neglected. To reveal whether the dimensionless number defined by Eq. (19) or its variant Eq. (20) is suitable for the present case, special figures of relation between the non-dimensional number M defined by Eq. (20) and tube wall thickness are shown in Fig. 7. Following two features may be noted from the four figures in Fig. 7. First for all the four subcases for k_{sf} = 1 the values of M are very small, which mean that the effect of the tube wall heat conduction can be neglected according to the definition of M. However, our results show that it is the cases with k_{sf} = 1 that tube wall heat conduction has its strong effect; second the values of M for k_{sf} = 25 are always larger than those of k_{sf} = 1. This means that relatively speaking for the cases of k_{sf} = 25 tube wall heat conduction has its effect according to the meaning of M. Our analysis gives the opposite judgment. Thus the dimensionless parameter defined by Eq. (19) or Eq. (20) is not suitable for the present study. The infeasibility of parameter M was also found in [23]. In [23] the single phase flow and heat transfer of water in microtubes with diameters from 120 to 528 μm were experimentally studied. The M values of the five cases studied were well below 10^{-2} (in order of 10^{-6} to 10^{-5}). However, axial heat conduction in tube was significant. These examples give us a hint: the criterion for judging the effect of wall axial heat conduction may be situation dependent. As indicated in [24], several criteria for judging the influence of wall heat conduction were proposed by different authors, including:

Faghri and Sparrow [7]:

$$M_{FS} = k_{sf}\frac{\delta}{R} \tag{23}$$

Cotton and Jackson [40]:

$$M_{CJ} = k_{sf}\left[\frac{\delta}{D_i}\left(1+\frac{\delta}{D_i}\right)\right]\frac{1}{Pe^2} \tag{24}$$

Chiou [41]:

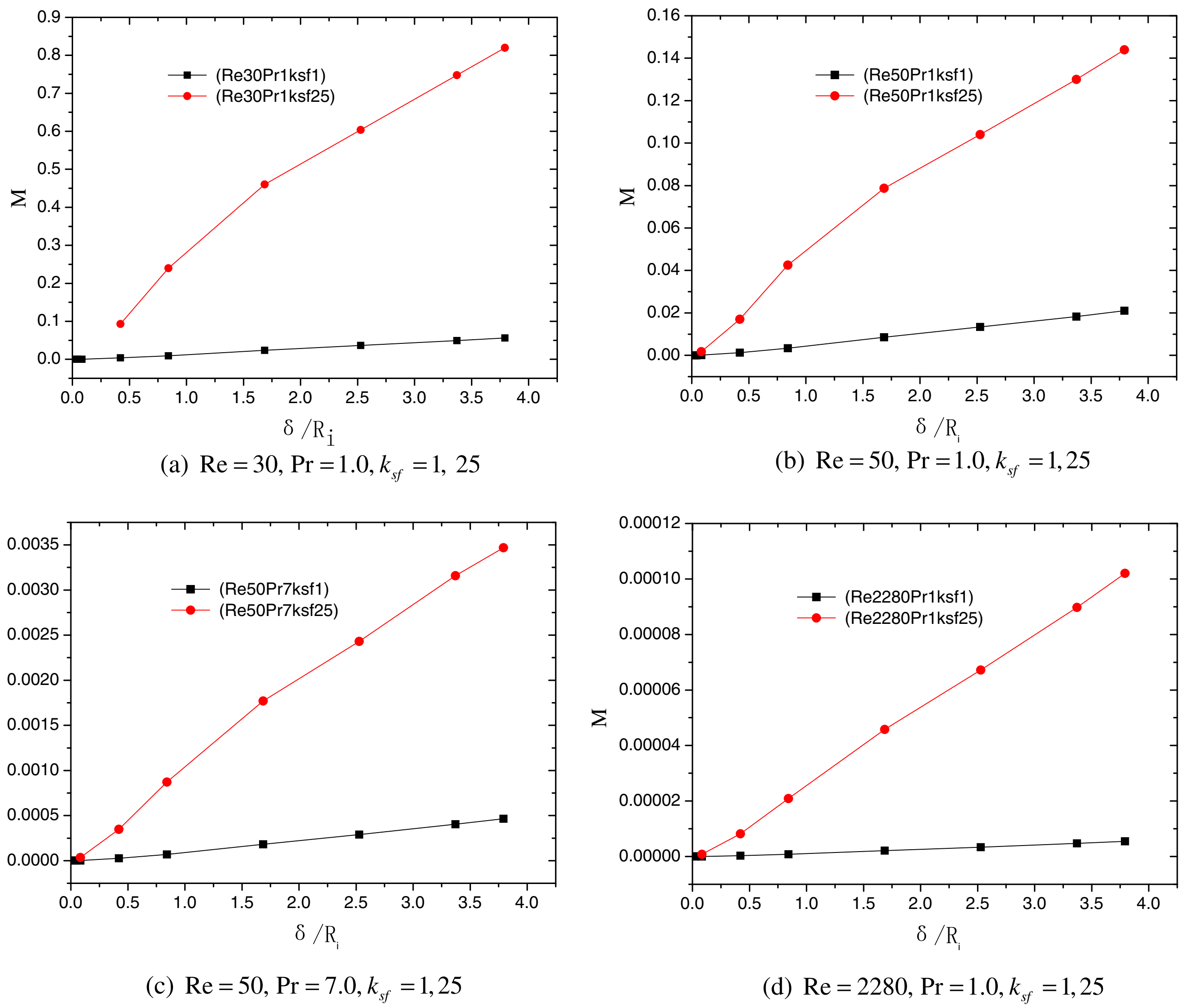

Fig. 7. Relation of the non-dimensional number (M) to tube wall thickness δ/R_i.

$$M_C = k_{sf}\frac{A_s}{A_f}\frac{D_i}{L}\frac{1}{Pe} \tag{25}$$

From Eqs. (19), (23)–(25), it can be found that most criteria include the ratio of thermal conductivities of wall solid and the fluids. For the problem studied in this paper it is likely that the predominant parameter for judging the effect of the wall axial heat conduction is the thermal conductivity ratio of wall over fluid.

Two more things are worth noting. First, the absolute value of M defined by Eq. (20) is different from that defined by Eq. (19). However, they are in the same order. Hence the above conclusion of the infeasibility of M is applicable to both definitions. Second, by "the effect of axial wall heat conduction" we actually mean that when a parameter related to the axial wall heat conduction changes, say k_{sf}, how significant is the change of the convective heat transfer characteristics. If the heat transfer characteristics are not affected by the variation of the component of axial wall heat conduction, we come to the conclusion that the axial wall heat conduction has no effect. Physically the larger the wall thermal conductivity, the stronger the axial heat conduction. For the problem studied in this paper, when the value of k_{sf} is larger than 25, the axial wall heat conduction is so strong that any change in the solid thermal conductivity will not influence the entire convective heat transfer characteristics. Such situation was also found in the conjugated heat transfer in eccentric annuli [42]. In [42] conjugated laminar forced convection heat transfer in the entry region of eccentric annuli is numerically investigated. Heat transfer parameters are presented for a fluid of Pr = 0.7 flowing in an annulus of radius ratio 0.5 for four values of dimensionless eccentricity ranging from 0.1 to 0.7. Solid–fluid conductivity ratio (k_{sf}) is varied to cover the range for practical cases with commonly encountered inner and outer tube thickness. Boundary conditions applied are isothermal heating of the inner surface of the core tube, while the outer surface of the external tube is maintained at the inlet fluid temperature. Limits for k_{sf} above which the effect of the axial wall heat conduction can be neglected are obtained. For example for the case of eccentricity $e = 0.1$, this limit is $k_{sf} = 17$.

4.3. Comparison with some other related results in references

To the authors' knowledge, among the results of existing literatures concerning the effect of axial wall heat conduction for the micochannels/tubes, the results by Guo and Li [15] are the most consistent with ours. As indicated above in their numerical analysis, the convective boundary condition was adopted at the outside surface of the tube, and numerical simulation was conducted by varying the surface convective resistance to wall conductance resistance. Their results show that the larger thermal conductivity ratio leads to a lower Nusselt number in the laminar fully developed region and the very low ratio approximates the constant wall heat flux condition. Since the effect of the axial heat conduction only one of their major concerns, no much detail were presented in their paper in this regard. As indicated above Patankar and Sparrow showed [16] that the external convective heat transfer condition has its two limiting cases: the negligible convective thermal resistance obtains the constant temperature result ($Nu = 3.66$) the negligible conduction resistance approaches the uniform heat flux condition (4.36). Our numerical results make a new contribution in this aspect: that for laminar flow in a thick-walled tube with constant outside surface temperature, the negligible axial wall heat conduction leads to the uniform surface temperature of the inner wall and the predominant axial heat conduction approximates the uniform heat flux at the tube inner surface.

5. Conclusions

A comprehensive numerical study of the simultaneously developing forced laminar flow and heat transfer in thick wall microtubes with constant outer wall temperature has been conducted by taking into account the conjugate effect of two-dimensional wall conduction and fluid axial conduction. Heat transfer characteristics are relied on four non-dimensional groups, Re, Pe(=RePr), k_{sf} and δ/R_i. Computations have been conducted in the following parameter ranges: $30 \leqslant \mathrm{Re} \leqslant 2280$, $1 \leqslant \mathrm{Pr} \leqslant 7$, $1 \leqslant k_{sf} \leqslant 10{,}000$, and $0 \leqslant \delta/R_i \leqslant 3.79$. The main conclusions are as follows:

(1) The influence of the ratio of wall thickness over tube diameter to forced laminar convection flow in a thick wall microtube strongly depends on the wall-to-fluid conductivity ratio k_{sf}.
(2) Under the conditions of $30 \leqslant \mathrm{RePr} \leqslant 11{,}560$ and $k_{sf} > 25$, the effects of wall thickness over tube diameter on the local Nusselt number, the thermal entrance length and the asymptotic Nusselt number can be neglected. The results about the thermal entrance length and the asymptotic Nusselt number are in good agreement with the results of convective heat transfer in a conventional tube with uniform inner wall surface.
(3) Under the conditions of $30 \leqslant \mathrm{RePr} \leqslant 11{,}560$ and $k_{sf} \leqslant 25$, the effects of wall thickness over tube diameter on the local Nusselt number, the thermal entrance length and the asymptotic Nusselt number must be considered. There is also the thermal developed region in the far downstream. But as the wall thickness over tube diameter increases, the thermal entrance length and asymptotic Nusselt number increase and are larger than those of convective heat transfer in a conventional tube with uniform inner wall surface. The maximum asymptotic Nusselt numbers obtained in this study is about 4.3. The maximum departure between the two thermal entrance lengths exceeds 20%.
(4) It is very likely that as the ratio of the wall thickness over tube diameter increases and the wall-to-fluid conductivity ratio k_{sf} decreases, the heat transfer in a thick-walled tube with constant outside wall temperature undergoes the transformation of the inner surface thermal boundary condition: from uniform temperature to uniform heat flux. It is similar to the laminar heat transfer in a thin-walled tube with the external convective boundary condition where the very large and very small external heat transfer coefficients correspond to the constant wall temperature and constant wall heat flux conditions, respectively.
(5) The basic function of the axial wall heat conduction, at least for the case studied, is to unify the heat flux at the inner wall surface. The criterion for judging the effect of the axial wall heat conduction may be problem-dependent, and M criterion proposed in [17] is not suitable for the analysis of thermally-developing fluid flow and heat transfer in microchannels/tubes with a fixed outer wall temperature.

Acknowledgments

This work was supported by the Key Project of the National and Natural Science Foundation of China (50636050) and the Key Project of Fundamental Research in China (G2007CB206902).

References

[1] L. Graetz, Uber die Warmeleifungsfahigkeit von Flussigkeiten, Part 1, Ann. Phys. Chem. 18 (1883) 79–94.
[2] L. Graetz, Uber die Warmeleifungsfahigkeit von Flussigkeiten Part 2, Ann. Phys. Chem. 25 (1885) 337–357.
[3] R.K. Shah, A.L. London, Laminar Flow Forced Convection in Ducts, Academic Press, New York, 1978. pp. 196–207.
[4] E.J. Davis, N.W. Gill, The effects of axial conduction in the wall on heat transfer with laminar flow, Int. J. Heat Mass Transfer 13 (1970) 459–470.
[5] S. Mori, M. Sakakibara, A. Tanimoto, Steady heat transfer to laminar flow in a circular tube with conduction in tube wall, Heat Transfer Jap. Res. 3 (1974) 3746–3751.
[6] S. Mori, T. Shinke, M. Sakakibara, A. Tanimoto, Steady heat transfer to laminar flow between parallel plates with conduction in wall, Heat Transfer Jap. Res. 5 (1976) 17–25.
[7] M. Faghri, E.M. Sparrow, Simultaneous wall and fluid axial conduction in laminar pipe-flow heat transfer, ASME J. Heat Transfer 102 (1980) 58–63.
[8] E.K. Zariffeh, H.M. Soliman, A.C. Trupp, The combined effects of wall and fluid axial conduction on laminar heat transfer in circular tubes, J. Heat Mass Transfer 4 (1982) 131–135.
[9] A. Campo, R. Rangel, Lumped system analyses for the simultaneous wall and fluid axial conduction in laminar pipe flow heat transfer, PhysicoChem. Hydrodyn. 4 (1983) 163–173.
[10] G.S. Barozzi, G. Pagliarini, A method to solve conjugate heat transfer problems: the case of fully developed laminar flow in a pipe, ASME J. Heat Transfer 107 (1985) 77–83.
[11] A. Campo, C. Shuler, Heat transfer in laminar flow through circular tubes accounting for two-dimensional wall conduction, Int. J. Heat Mass Transfer 31 (1988) 2251–2259.
[12] S. Bilir, Laminar flow heat transfer in pipes including two-dimensional wall and fluid axial conduction, Int. J. Heat Mass Transfer 38 (9) (1995) 1619–1625.
[13] C.M. Ho, Y.-C. Tai, Micro-electronic mechanic systems (MEMS) and fluid flows, Ann. Rev. Fluid Mech. 30 (1998) 5–33.
[14] M. Gad-el-Hak, The fluid mechanics of micro-devices. The Freeman Scholar lecture, J. Fluid Eng. 121 (1999) 5–33.
[15] Zeng-Yuan Guo, Zhi-Xin Li, Size effect on single-phase channel flow and heat transfer at microscale, Int. J. Heat Fluid Flow 24 (2003) 284–298.
[16] E.M. Sparrow, S.V. Patankar, Relationship among boundary conditions and Nusselt number for thermally developed duct flow, ASME J. Heat Transfer 99 (1977) 483–485.
[17] G. Maranzana, I. Perry, D. Maillet, Mini- and microchannels: influence of axial conduction in the walls, Int. J. Heat Mass Transfer 47 (2004) 3993–4004.
[18] J. Zueco, F. Alhama, C.F. González Fernández, Analysis of laminar forced convection with network simulation in thermal entrance region of ducts, Int. J. Therm. Sci. 43 (2004) 443–451.
[19] I. Tiselj, G. Hetsroni, B. Mavko, A. Mosyak, E. Pogrebnyak, Z. Segal, Effect of axial conduction on the heat transfer in micro-channels, Int. J. Heat Mass Transfer 47 (2004) 2551–2565.
[20] Gabriel Gamrat, Michel Favre-Marinet, Dariusz Asendrych, Conduction and entrance effects on laminar liquid flow and heat transfer in rectangular microchannels, Int. J. Heat Mass Transfer 48 (2005) 2943–2954.
[21] G. Hetsroni, A. Mosyak, E. Pogrebnyak, L.P. Yarin, Heat transfer in microchannels: comparison of experiments with theory and numerical results, Int. J. Heat Mass Transfer 48 (2005) 5580–5601.
[22] Roland Bavière, Michel Favre-Marinet, Ste'phane Le Person, Bias effects on heat transfer measurements in microchannel flows, Int. J. Heat Mass Transfer 49 (2006) 3325–3337.
[23] G.P. Celata, M. Cumo, V. Marconi, S.J. McPhail, G. Zummo, Microtube liquid single-phase heat transfer in laminar flow, Int. J. Heat Mass Transfer 49 (2006) 3538–3546.
[24] D. Lelea, The conjugate heat transfer of the partially heated microchannels, Heat Mass Transfer 44 (2007) 33–41.
[25] Z. Li, G.H. Tang, Y.L. He, W.Q. Tao, Experimental and numerical studies of liquid flow and heat transfer in microtubes, Int. J. Heat Mass Transfer 50 (2007) 3447–3460.
[26] Zhigang Liu, Yaohua Zhao, Masahiro Takei, Experimental study on axial wall heat conduction for convective heat transfer in stainless steel microtube, Heat Mass Transfer 43 (2007) 587–594.

[27] B. Weigand, G. Gassner, The effect of wall conduction for the extended Graetz problem for laminar and turbulent channel flows, Int. J. Heat Mass Transfer 50 (2007) 1097–1105.
[28] Weilin Qu, Issam Nudawar, Analysis of three-dimensional heat transfer in micro-channel heat sinks, Int. J. Heat Mass Transfer 45 (2002) 935–937.
[29] K.C. Toh, X.Y. Chen, J.C. Chai, Numerical computation of fluid flow and heat transfer in microchannels, Int. J. Heat Mass Transfer 45 (2002) 5133–5141.
[30] H. Herwig, O. Hausner, Critical view on "new results in micro-fluid mechanics": an example, Int. J. Heat Mass Transfer 46 (5) (2003) 935–937.
[31] S.V. Patankar, Numer. Heat Transfer Fluid Flow, Hemisphere, Washington, DC, 1980.
[32] W.Q. Tao, Numerical Heat Transfer, second ed., Xi'an Jiaotong University Press, Xi'an, 2001.
[33] Z.Y. Li, W.Q. Tao, A new stability-guaranteed second-order difference scheme, Numer. Heat Transfer– Part B 42 (4) (2002) 349–365.
[34] J.P. Van Doormaal, G.D. Raithy, Enhancements of the simple method for predicting incompressible fluid flows, Numer. Heat Transfer – Part B 7 (2) (1984) 147–163.
[35] L.C. Burmerister, Convective Heat Transfer, John Weily & Sons, 1983.
[36] P. Sharath, C. Rao, M. Rahman, H. Soliman, Numerical simulation of steady-state conjugate heat transfer in a circular microtube inside a rectangular substrate, Numer. Heat Transfer – PartA 49 (2006) 635–654.
[37] D. Lelea, S. Nisheo, K. Takano, The experimental research on microheat transfer and fluid flow of distilled water, Int. J. Heat Mass Transfer 47 (2004) 2817–2830.
[38] H. Yapici, B. Albayrak, Numerical solution of conjugate heat transfer and thermal stresses in a circular pipe externally heated with non-uniform heat flux, Energy Convers. Manage. 45 (2004) 927–973.
[39] P.-S. Lee, S. Garimella, D. Liu, Investigation of heat transfer in rectangular microchannels, Int. J. Heat Mass Transfer 48 (2005) 1688–1704.
[40] M.A. Cotton, J.D. Jackson, The effect of heat conduction in a tube upon forced convection heat transfer in the thermal entrance region, in: Numerical Methods in Thermal Problems, vol. iv, Pinerige Press, Swansea, 1985, pp. 504–515.
[41] J.P. Chiou, The advancement of compact heat exchanger theory considering the effects of longitudinal heat conduction and flow nonuniformity, in: R.K. Shah, C.F. McDonald, C.P. Howard (Eds.), Symposium on Compact Heat Exchangers—History, Technological Advancement and Mechanical Design Problems, HTD, vol. 10, ASME, New York, 1980, pp. 101–121, Book No. G00183.
[42] M.A.E. El-Shaarawi, S.A. Haider, Critical conductivity ratio for conjugate heat transfer in eccentric annuli, Int. J. Numer. Methods Heat Fluid Flow 11 (2001) 255–279.